# Calorimetric and Magnetic Studies of Crystalline and Glassy Bis[*N*-(3-methoxysalicylidene)isopropylamine]nickel(II)[1]

Naoto Arai, Michio Sorai, and Syûzô Seki

*Department of Chemistry, Faculty of Science, Osaka University, Toyonaka, Osaka*

(Received March 1, 1972)

Thermal and magnetic properties of Ni(3-$CH_3O$-SAL·*iso*-$C_3H_7$)$_2$ were investigated by measuring thermograms, infrared and electronic spectra, heats of solution, magneitc susceptibilities, and heat capacities around glass transition temperature. In addition to the known paramagnetic crystalline phase III and the diamagnetic crystalline phase IV, two new crystalline phases (I and II) were discovered. Phase I was found to be paramagnetic, its molecular geometry being of a tetrahedral four-coordinated form like that of phase III, while phase II, similar to phase IV, is diamagnetic and has a square-planar four-coordinated form. Although the order of thermodynamic stability of these four crystalline phases was not determined, they were isolated stably at room temperature. The supercooled liquid and glassy states of this compound were realized for the first time by quenching the sample in the molten state. Unusual magnetic behaviors of these two states were satisfactorily accounted for by assuming an equilibrium between the diamagnetic and the paramagnetic species. In the supercooled liquid state, the paramagnetic species was partially converted into the diamagnetic one with decreasing temperature. Below the glass transition temperature $T_g$, however, this conversion process was prevented and the magnetic susceptibility obeyed apparently Curie's law with a 26% paramagnetic content. The heat capacity measurement revealed a typical glass transition phenomenon at 297.5 K and the heat capacity jump at $T_g$ was determined to be 172 $JK^{-1}mol^{-1}$. Detailed discussions were given for the relationship between molecular geometry and its associated magnetic property and also for the phase relationship between various phases.

Extensive studies have been carried out on the magnetic properties of the Schiff base metal complexes. An interesting problem in this field might be the elucidation of the relationship between the geometry of molecules and their associated magnetic properties. Bis(*N*-R-X-salicylidene)nickel(II) is a typical example. The molecular formula of this compound is illustrated in Fig.1 and abbreviated as Ni(X-SAL·R)$_2$

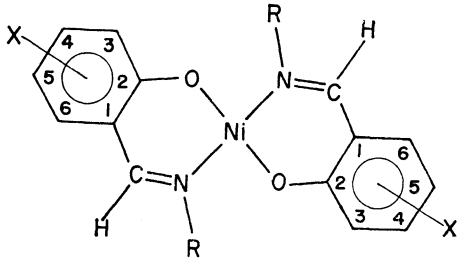


Fig. 1. Molecular formula of Ni(X-SAL·R)$_2$.

hereafter. By varying the substituent groups X and/or R, this coordination compound can possess the following four molecular forms; (i) square planar four-coordinated form, (ii) tetrahedral four-coordinated one, (iii) binuclear five-coordinated one, and (iv) polymeric octahedral six-coordinated chain form.[2-4]

In the solutions in inert solvents, Ni(X-SAL·R)$_2$ exists as an equilibrium mixture consisting of two or more species of the four forms. The magnetic properties of these solutions depend on both temperature and concentration. This phenomenon is well known as "solution paramagnetism."

In a solid state, however, a given Ni(X-SAL·R)$_2$ can possess only one form. Rare exceptions are the cases of Ni(H-SAL·$CH_3$)$_2$,[5,6] Ni(5-Cl-SAL·$CH_3$)$_2$,[7] and Ni(5-Br-SAL·$CH_3$)$_2$,[7] where the additional paramagnetic forms have been obtained by heating the stable diamagnetic form in a solid state.

Recently Yamada *et al.*[8] reported the new finding of a pair of isomers for crystalline Ni(3-$CH_3O$-SAL·*p*-Cl-$C_6H_4$)$_2$ and Ni(3-$CH_3O$-SAL·*p*-Br-$C_6H_4$)$_2$, where the binuclear five-coordinated as well as the polymeric six-coordinated forms have been stably isolated as a crystalline state. A similar isolation has been also reported for the present material by the same authors [9] In this case brown and green crystals were obtained from methanol and ethylether solutions, respectively. The electronic spectra and magnetic susceptibility measurements at room temperature revealed that the brown crystal shows paramagnetism and its central $Ni^{2+}$ ion is coordinated tetrahedrally, while the green crystal is diamagnetic with a square-planar form. These authors also reported transformation of the green form into the brown one at 430—431 K followed by melting at 460—461 K.

The main purpose of the present work is to investigate the relationship between molecular geometry and magnetism in Ni(3-$CH_3O$-SAL·*iso*-$C_3H_7$)$_2$ and also to elucidate the relative thermodynamic stability among different crystalline forms by means of precise heat of solution and magnetic susceptibility measurements as well as spectroscopic methods. In addition to the green and the brown forms mentioned above, we found two other new crystalline phases which exist stably at room temperature. We also found that both the supercooled liquid and the glassy states can

1) A part of this paper was read before the 6th Japanese Calorimetry Conference, November (1970), Yokohama.

2) R. H. Holm, G. W. Everett, Jr., and A. Chakarvorty, *Progr. Inorg. Chem.*, **7**, 83 (1966).

3) B. O. West, "New Pathways in Inorganic Chemistry," Cambridge Univ. Press (1968), p. 303.

4) E. K. Barefield and D. H. Busch, *Quart. Rev.*, **22**, 456 (1968).

5) C. M. Harris, S. L. Lenzer, and R. L. Martin, *Austral. J. Chem.*, **11**, 331 (1958).

6) L. Sacconi, P. Paoletti, and R. Cini, *J. Amer. Chem. Soc.*, **80**, 3583 (1958).

7) H. C. Clark and R. J. O'Brien, *Can. J. Chem.*, **37**, 436 (1959); **39**, 1030 (1961).

8) S. Yamada, K. Iwasaki, and A. Takeuchi, *Inorg. Chim. Acta*, **2**, 395 (1968).

9) A. Takeuchi and S. Yamada, This Bulletin, **42**, 3046 (1969).

be realized by quenching the molten state. The brown and green forms will be designated as crystalline phases III and IV, respectively, and the two new forms as crystalline phases I and II, respectively, following the order of magnitude of heat of solution of each phase (see Fig.5).

For the sake of comparison, the magnetic structure of Ni(H-SAL·$CH_3)_2$ crystal was also investigated by measuring the infrared and electronic spectra as well as the thermograms.

## Experimental

*Material.* *(A) Ni(3-$CH_3O$-SAL·iso-$C_3H_7)_2$*: Of the four isomers of the present complex, crystalline phases III and IV were prepared by following the method of Takeuchi and Yamada[9] and phases I and II were obtained from III or IV on heating in the solid state. Preparation of each crystalline phase, the supercooled liquid and the glassy state was carried out as follows:

*(i) Crystalline phase III.* The crude material was recrystallized from methanol solution to give brown prism crystals.

*(ii) Crystalline phase IV.* Evaporation of a solvent from a green ethylether solution of the brown crystal yielded a green prism crystal which was purified by recrystallization from the same solvent.

*(iii) Crystalline phase I.* Heating the crystalline phase III up to 443—448 K for *ca.* 15 minutes or phase IV up to 403—438 K for *ca.* 30 minutes under the atmosphere of helium gas converted the respective phases into a brown colored phase I, which was easily supercooled down to room temperature.

*(iv) Crystalline phase II.* By keeping the supercooled liquid of the present complex at 343—363 K for *ca.* 30 minutes, crystallization took place to give a green solid phase II, which was also supercooled easily to room temperature.

*(v) Supercooled liquid and glassy states.* These phases were obtained by quenching the molten substance at a cooling rate greater than 10 K $min^{-1}$. Results of chemical and elementary analyses of each crystalline phases are given in Table 1.

Table 1. Elementary and chemical analyses of Ni(3-$CH_3O$-SAL·*iso*-$C_3H_7)_2$ and Ni(H-SAL·$CH_3)_2$

| | | C(%) | H(%) | N(%) | Ni(%) |
|---|---|---|---|---|---|
| | Ni(3-$CH_3O$-SAL·*iso*-$C_3H_7)_2$ | | | | |
| Calcd | | 59.62 | 6.37 | 6.32 | 13.25 |
| Found | Phase I | 59.49 | 6.28 | 6.32 | — |
| | Phase II | 59.67 | 6.39 | 6.29 | — |
| | Phase III | 59.75 | 6.47 | 6.34 | 13.16 |
| | Phase IV | 59.70 | 6.37 | 6.32 | — |
| | Ni(H-SAL·$CH_3)_2$ | | | | |
| Calcd | | 58.77 | 4.93 | 8.57 | 17.95 |
| Found | Phase I | 58.61 | 4.94 | 8.56 | 17.83 |
| | Phase II | 58.73 | 4.95 | 8.56 | 17.82 |

*(B) Ni(H-SAL·$CH_3)_2$*: Diamagnetic green form (phase II) and paramagnetic buff-colored form (phase I) were prepared according to the methods by Klemm and Raddatz[10] and others.[5,6] The results of elementary and chemical analyses of both forms are also shown in Table 1.

*Thermal Analysis.* Prior to precise calorimetric investigation, thermal analysis was made by using a differential scanning calorimeter (Perkin-Elmer, DSC-1B) at 173—473 K. The scanning rate was 10 K $min^{-1}$.

*Infrared Absorption Spectra.* The infrared spectra of Ni(3-$CH_3O$-SAL·*iso*-$C_3H_7)_2$ and Ni(H-SAL·$CH_3)_2$ were recorded on a Grating-type Infrared Spectrophotometer Model DS-402G (Japan Spectroscopic Co., Ltd.) in the range 4000—400 $cm^{-1}$ at room temperature and 120 K. The far-infrared spectra of both compounds were also obtained by a Spectrophotometer No.FIS-001(Hitachi Ltd.) in the range 500—80 $cm^{-1}$ at the same temperatures. The Nujol mull method was employed for preparation of the samples.

*Electronic Spectra.* In order to get more insight into the coordination schemes in each phase of Ni(3-$CH_3O$-SAL·*iso*-$C_3H_7)_2$ we measured the electronic spectra. For the sake of comparison the electronic spectra of Ni(H-SAL·$CH_3)_2$ were also measured. The electronic reflection spectra of both compounds in solid state were recorded on a spectrophotometer model EPU-2A (Hitachi Ltd.) in the range 23,000—10,000 $cm^{-1}$ at room temperature.

*Heat of Solution.* The heat of solution of Ni(3-$CH_3O$-SAL·*iso*-$C_3H_7)_2$ into chloroform was measured by using a LKB-8700 Precision Calorimetry System at 18—30°C. The calorimeter was standardized on an international scale in our laboratory by measuring the heat of solution of tris(methylhydroxy)aminomethane into 0.1 N HCl solution. The amount of sample used in each measurement varied from 90 to 620 mg but the amount of solvent was always about 100 $cm^3$.

*Heat Capacity.* The heat capacities of phase II and the glassy state of Ni(3-$CH_3O$-SAL·*iso*-$C_3H_7)_2$ at 230—343 K were measured by using an adiabatic calorimeter.[11] The amount of specimen was 24.3532 g(=0.0549502 moles). A small quantity of helium gas was sealed into the calorimeter cell along with the sample to aid in the heat transfer. The experimental errors were within ±0.3% in all cases.

The glassy state was prepared by quenching the molten substance in the calorimeter cell to dry-ice temperature. In this case the cooling rate was estimated to be about −100 K $min^{-1}$. After quick setting of the calorimeter cell to the cryostat, the temperature of the cell was maintained at 273 K during the course of evacuation of the equipment. This procedure prevented the transformation of the supercooled liquid into phase II.

The sample of phase II was prepared by complete transformation of the supercooled liquid into this phase by keeping the sample at 339.4 K(just above the crystallization temperature) for *ca.* 12 hr.

*Magnetic Susceptibility.* The magnetic susceptibilities of Ni(3-$CH_3O$-SAL·*iso*-$C_3H_7)_2$ were measured at the field-strength of 7.65 kG by use of the Faraday method in the temperature region 120—530 K. The amount of specimen employed was 400—500 mg.

## Phase Relationships

Thermal analysis is one of the most effective methods for determining phase relations. Run 1 in Fig.2 shows the DSC curve of the brown paramagnetic phase III of Ni(3-$CH_3O$-SAL·*iso*-$C_3H_7)_2$. In heating direction the DSC curve showed an endothermic peak with a small subsequent exothermic effect at 433—443 K. Phase III was transformed into a new high-temperature phase. This phase (mp 460 K) was easily supercooled down to 173 K (see Run 2). The thermal behavior of the green phase IV is shown in Run 3. Phase IV was transformed into a high-temperature phase at 383 K, which was also supercooled down to 173 K and

10) W. Klemm and K. H. Raddatz, *Z. Anorg. Allgem. Chem.*, **250**, 207 (1942).

11) H. Suga and S. Seki, This Bulletin, **38**, 1000 (1965).

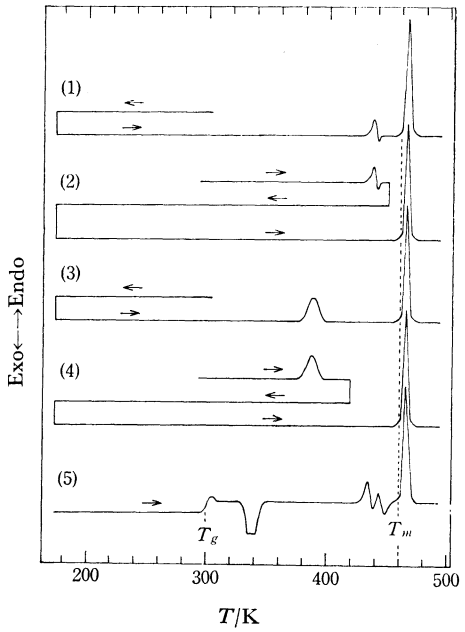


Fig. 2. DSC curves; (1) phase III, (2) a new high-temperature phase obtained from phase III, (3) phase IV, (4) a new high-temperature phase obtained from phase IV, and (5) the glassy state.

melted at 460 K (see Run 4). The thermal behavior of the molten substance of phase IV was exactly the same as that of phase III. By cooling the molten substance at the rate $-10$ K min$^{-1}$ the liquid state was quenched to the lowest temperature investigated. Run 5 shows the heating curve of the quenched substance, which exhibited a thermal anomaly similar to that in a glass transition at *ca.* 298 K. The anomaly was confirmed to be a real glass transition through the enthalpy relaxation effects observed by auxiliary experiments. On further heating an exothermic peak due to crystallization was observed at *ca.* 333 K where the supercooled liquid state was irreversibly transformed into another crystalline phase, which we designate crystalline phase II. The phase showed rather complicated thermal behaviors at 423—453 K and melted at 460 K. It should be noticed that both high-temperature phases obtained by heating phases III and IV were recognized as the same crystalline phase, which we designate crystalline phase I. The colors of phases I and II were brown and green, respectively.

Infrared absorption spectra can provide useful information on molecular structure. Although quantitative assignments have not been made, noticeable differences in absorption peaks were observed among each crystalline phases. In the case of Ni(3-$CH_3O$-SAL·*iso*-$C_3H_7)_2$, the infrared spectrum of phase I was, on the whole, similar to that of phase III. However, extra absorption peaks characteristic of phase I were observed especially in the range 800—700 cm$^{-1}$ and at 1045 cm$^{-1}$. The spectra of phases II and IV, on the other hand, resembled each other except for a slight differences in the range 400—350 cm$^{-1}$. The spectra of phases I and III were, however, quite unlike those of II and IV. The four spectra might be grouped into two classes, one consisting of the spectra of phases I and III, and the other the spectra of phases II and IV. One of the most characteristic peaks which can be distinguished from

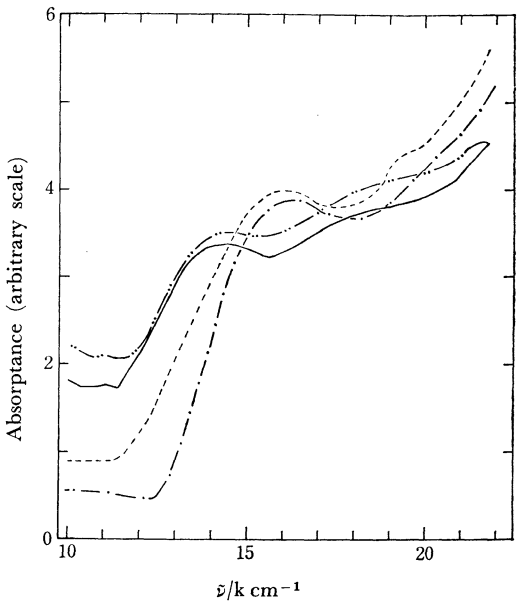


Fig. 3. The electronic spectra at room temperature; ——, phase I; – – –, phase II; —·—, phase III; —··—, phase IV.

each class is the C=N stretching vibration near 1600 cm$^{-1}$. The single peak due to the C=N stretching in the first class was found to split into a doublet in the case of the second class; *i. e.*, 1607 cm$^{-1}$ (strong) for phase I; 1607 cm$^{-1}$ (strong) for phase III; 1602 (shoulder) and 1615 cm$^{-1}$ (strong) for phase II; 1603 (moderate) and 1622 cm$^{-1}$ (strong) for phase IV. Another characteristic band probably due to one of the metal-ligand coordinate bonds appeared in the far-infrared region; 304 cm$^{-1}$ (phase I), 346 cm$^{-1}$ (phase II), 301 cm$^{-1}$ (phase III), and 347 cm$^{-1}$ (phase IV).

In general, infrared spectra reflect the difference in molecular structure as well as the local symmetry in which a relevant absorption mode will be excited. Appreciable differences observed between the two classes indicate that remarkable differences exist in the molecular structure and the local symmetry. There is, however, little distinction between phases I and III and also between II and IV.

Similar situations were also observed in the electronic spectra of the four crystalline phases. The electronic spectra of Ni(3-$CH_3O$-SAL·*iso*-$C_3H_7)_2$ at room temperature are shown in Fig.3. The absorption maxima due to the crystal-field bands appeared at 11100 (weak), 14330 (strong), and 17830 cm$^{-1}$ (broad) for phase I and at 11050 (weak), 14500 (strong), and 18300 cm$^{-1}$ (broad) for phase III. These spectra have the closest resemblance to those of the other Schiff base nickel complexes with tetrahedral configuration. On the other hand, phases II and IV showed the crystal-field band at 16000 cm$^{-1}$ and at 16200 cm$^{-1}$, respectively. These features are similar to the spectrum of the square planar phase II in Ni(H-SAL·$CH_3)_2$. It is therefore safely concluded that the coordination scheme in phases I and III of Ni(3-$CH_3O$-SAL·*iso*-$C_3H_7)_2$ is tetrahedral and in phases II and IV square planar.

## Heat of Solution

If the precise heat capacity data from sufficiently

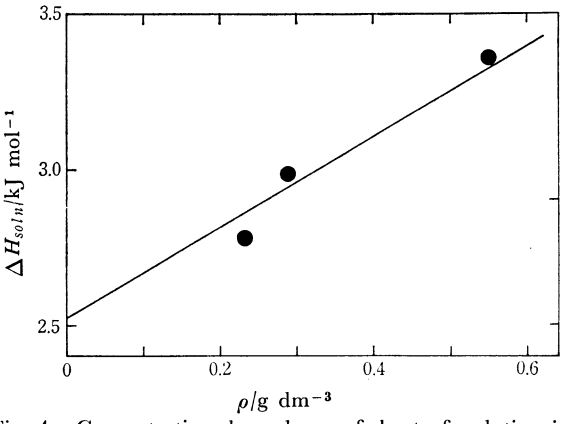


Fig. 4. Concentration dependence of heat of solution into chloroform at 24°C.

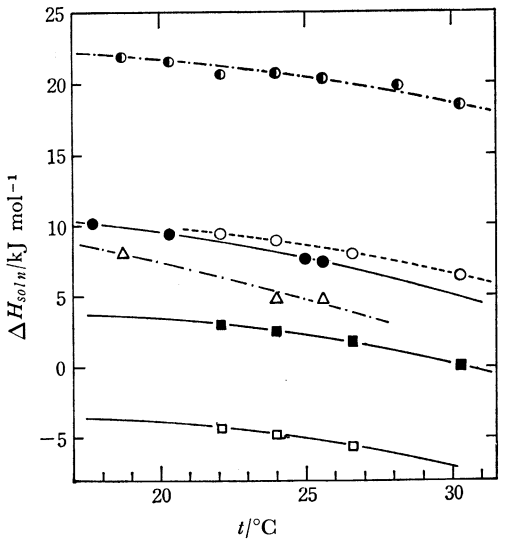


Fig. 5. Temperature dependence of the heat of solution; ○, phase I obtained from phase III; ●, phase I obtained from phase IV; △, phase II; ■, phase III; □, phase IV; and ◐, supercooled liquid state.

low temperatures are combined with the data of heat of solution, the difference in standard Gibbs energy between the phases might be obtained. The values enable us to determine the order of thermodynamic stability among various crystalline phases which remain "stable" at room temperature. We have measured the heat of solution of four crystalline phases and the supercooled liquid state of Ni(3-$CH_3O$-SAL·*iso*-$C_3H_7)_2$ at 18–30 °C. In order to confirm a possible concentration dependence on the heat of solution in advance, the data for the brown phase III was measured at 24°C by varying the amount of specimen. As is shown in Fig.4, an approximately linear dependence exists in the concentration region investigated. In determining the heat of solution, the following two assumptions were made; (i) the final state of the solution is identical in all cases and (ii) the correction to the infinitely diluted state of any sample is regarded as the same as the result given in Fig.4. The heats of solution thus obtained for each phase and the supercooled liquid state are plotted in Fig.5 as a function of temperature. The experimental error was estimated to be within ±0.62%. The ordinate $\Delta H_{soln}$ corresponds to the enthalpy difference between the infinitely diluted solution and solid phase.

We have regarded two high-temperature phases obtained by heating both phases III and IV as the identical phase (phase I), based on the results of infrared spectra. It was found, however, that there exists a slight but significant discrepancy in the heat of solution between the two kinds of samples of phase I prepared from phases III and IV (Fig.5). The discrepancies are beyond experimental error. This could be accounted for by close examination of each transition behavior revealed by the DSC curves. As shown in Fig.2, phase IV is transformed into phase I at 383 K accompanied by an endothermic peak, while phase III is transformed into phase I at a higher temperature *via* a metastable phase. The endothermic peak at 433 K corresponds to the transition from phase III to a metastable phase and the subsequent exothermic peak corresponds to that of metastable phase to phase I. In this two-step transition a sintering phenomenon was observed directly in the sample glass tube. The temperature range for phase I obtained from phase III is quite narrow compared with that formed from phase IV. Thus, severe control of temperature and complete transformation are necessary for the preparation of pure and stable phase I from phase III. The differences in the heat of solution of phase I can be attributed to the incomplete transformation from a metastable phase to phase I.

On the other hand, the heat of solution data for a supercooled liquid state and for phase II is not so accurate compared with those for phases I, III, and IV for the following reasons. The heat capacity measurement revealed that partial crystallization occurred in the supercooled liquid region even at temperatures far below the exothermic peak in the DSC curve. Thus the supercooled liquid samples used for the measurement of heat of solution seem to involve a certain amount of phase II arising from a partial crystallization at these temperatures, while the samples of phase II can involve partially the supercooled liquid state since the crystallization was too sluggish to attain completion.

It should be pointed out that there is a fundamental difference between thermal and various spectroscopic investigations. Only a slight difference was observed between phases I and III, and also between phases II and IV both in the infrared as well as in the electronic spectra. We have thus grouped these four phases into two classes; one consisting of phases I and III with the tetrahedral molecular form and the other of phases II and IV with the square-planar molecular form. The heat of solution, however, revealed large differences between phases I and III, and also between phases II and IV. These results imply that thermal investigations such as the measurement of heat of solution are more useful than spectroscopic analysis in the study of intermolecular interaction in relation to molecular arrangement or phase problem in the solid state.

## Heat Capacity around Glass Transition Temperature

In order to obtain more quantitative insight into the glass transition phenomenon, the heat capacities

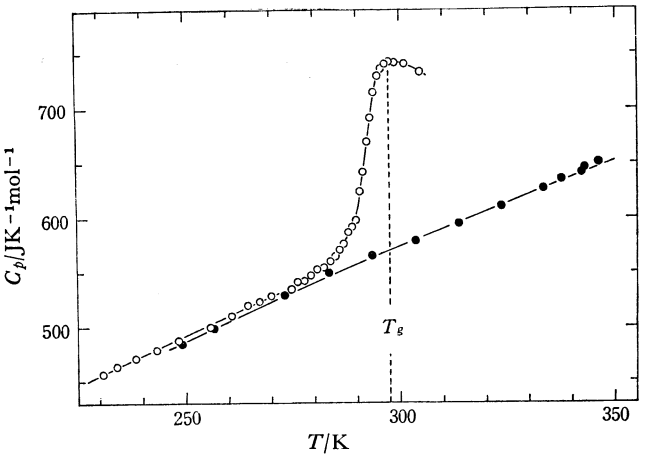


Fig. 6. Heat capacity around $T_g$; ○, glassy state and ●, phase II.

Table 2. The heat capacity of Ni(3-$CH_3O$-SAL·*iso*-$C_3H_7)_2$ (Molecular weight 443.187)

| $T$/K | $C_p$/J K$^{-1}$mol$^{-1}$ | $T$/K | $C_p$/J K$^{-1}$mol$^{-1}$ |
|---|---|---|---|
| Glassy state | | 292.374 | 670.11 |
| 230.747 | 457.22 | 293.229 | 691.80 |
| 233.948 | 463.53 | 294.072 | 715.63 |
| 238.278 | 470.86 | 294.925 | 730.23 |
| 243.188 | 479.28 | 295.784 | 736.37 |
| 248.349 | 487.84 | 296.645 | 740.75 |
| 255.724 | 499.94 | 297.614 | 743.28 |
| 260.712 | 510.34 | 299.010 | 741.87 |
| 264.548 | 519.72 | 301.359 | 740.91 |
| 267.276 | 523.23 | 304.847 | 733.60 |
| 269.982 | 527.98 | 337.524 | 635.09 |
| 272.827 | 530.73 | 342.273 | 641.37 |
| 274.666 | 534.66 | 346.030 | 650.56 |
| 276.198 | 541.15 | | |
| 277.722 | 542.11 | | |
| 279.238 | 547.13 | Phase II | |
| 280.745 | 552.55 | 249.000 | 484.78 |
| 282.237 | 554.30 | 256.506 | 499.93 |
| 283.715 | 559.98 | 264.139 | 504.20 |
| 284.930 | 564.47 | 273.187 | 529.05 |
| 285.903 | 570.49 | 283.473 | 549.43 |
| 286.879 | 576.29 | 293.502 | 565.19 |
| 287.845 | 587.17 | 303.569 | 578.93 |
| 288.799 | 591.66 | 313.699 | 594.67 |
| 289.732 | 598.35 | 323.651 | 611.00 |
| 290.639 | 624.30 | 333.426 | 626.95 |
| 291.527 | 642.05 | 343.002 | 646.12 |

of the glassy state and phase II were measured at 230—343 K. The results are plotted in Fig .6 and listed in Table 2. A typical glass transition was observed at 297.5 K. The ratio of the glass transition temperature $T_g$ to the melting point amounted to 0.648. This value falls within the range 0.50—0.67, which is favorable to a number of glass-forming materials. The heat capacity jump $\Delta C_p$ at $T_g$ was 172 JK$^{-1}$mol$^{-1}$ and the ratio of $\Delta C_p$ to the heat capacity of phase II at this temperature was found to be 0.309. The exothermic effect due to crystallization was observed just above $T_g$ and the heat capacity in the narrow supercooled liquid region decreased with increasing temperature, even after correction of a temperature drift in the computation of the heat capacities. We were not able to measure the heat capacity of the supercooled liquid state above 305 K because the great evolution of heat due to the crystallization effect disturbed the measurements. Due to this gradual heat evolution effect even above $T_g$, we were not able to estimate the heat of crystallization directly from the heat capacity data. We can, however, evaluate this heat effect from the difference of heats of solutions for phase II and supercooled liquid state which amounts to *ca.* 15.7 kJ mol$^{-1}$.

## Magnetic Properties

Extensive studies have been carried out on the magnetic susceptibility measurements of the Schiff base metal complexes. However, almost all the data are restricted to those obtained at room temperature. More quantitative information on the magnetic properties could be provided by varying the temperature.

We measured the magnetic susceptibility of the various phases of Ni(3-$CH_3O$-SAL·*iso*-$C_3H_7)_2$ over a wide temperature range of 120—530 K. The molar susceptibilities $\chi_m$ are plotted in Figs. 7—10. To make clear their correspondence to thermal behaviors, the results of DSC curves are also given. Although the general aspect of magnetic susceptibility coincided with the results of thermal data, slight mismatches in some anomalous parts were observed because of the different scanning rate of temperature, *i.e.*, 4—6 K min$^{-1}$ in the magnetic measurement and 10 K min$^{-1}$ in the thermal analysis, and also because of the uncertainty involved in temperature measurement for

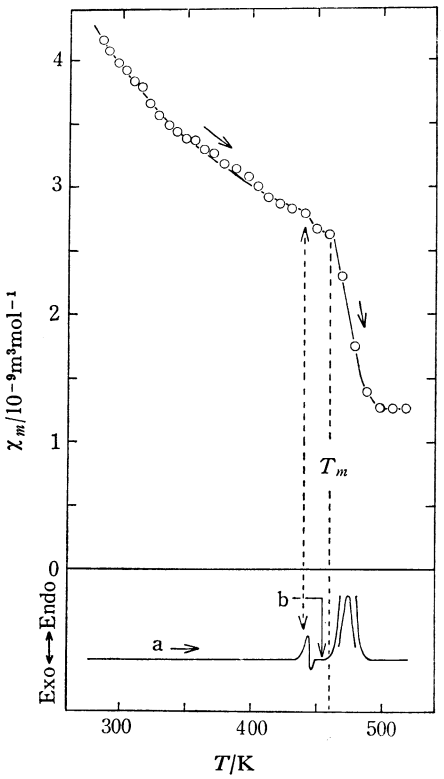


Fig. 7. Magnetic susceptibility $\chi_m$ *versus* temperature for phase III; (a) phase III and (b) phase I. In this and in Figs. 8—10, the DSC curves are also shown for comparison.

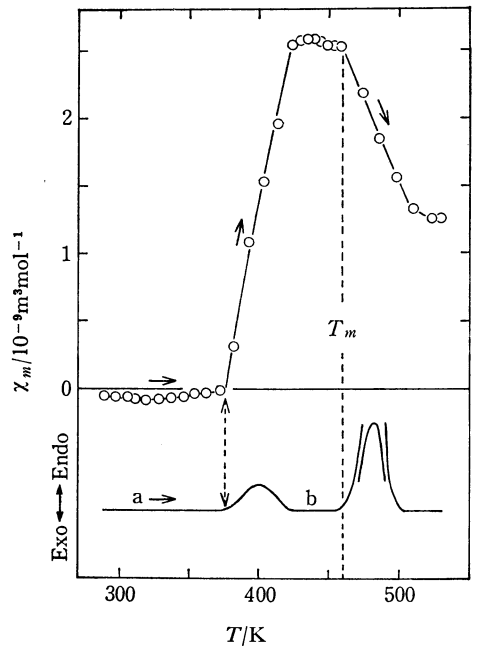


Fig. 8. $\chi_m$ *versus* $T$ for phase IV; (a) phase IV and (b) phase I.

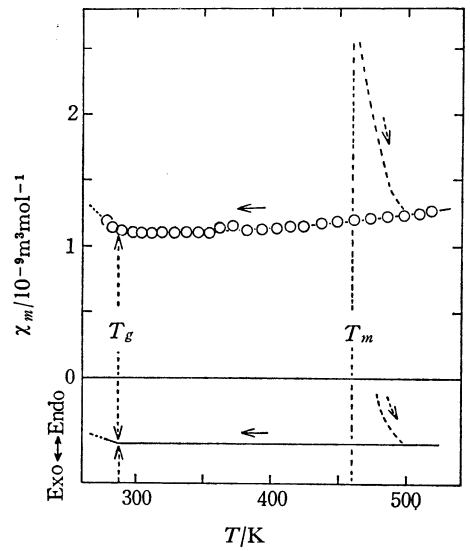


Fig. 9. $\chi_m$ *versus* $T$ for supercooled liquid state.

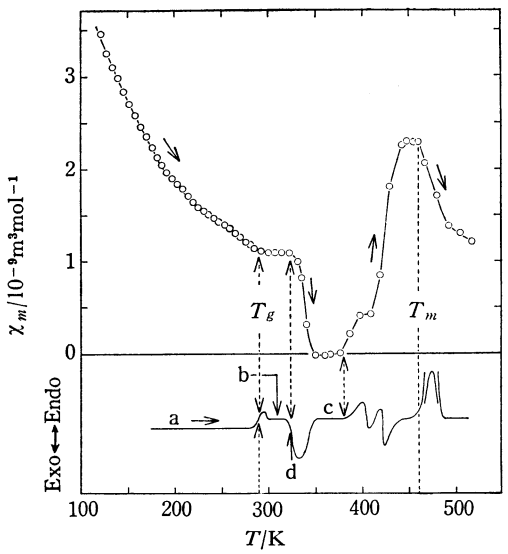


Fig. 10. $\chi_m$ *versus* $T$ for the glassy state; (a) glassy state, (b) supercooled liquid state, (c) phase II, and (d) crystallization.

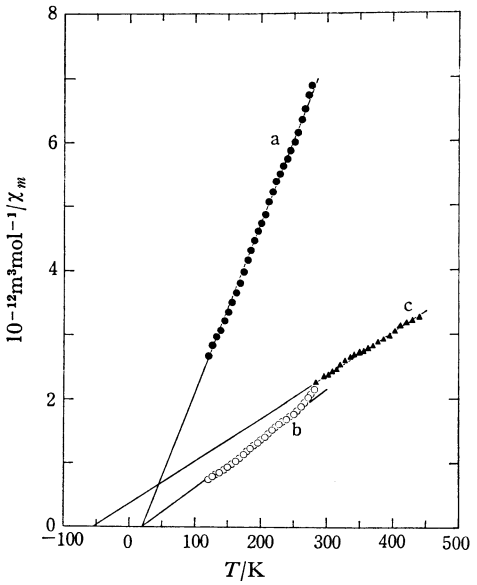


Fig. 11. $1/\chi_m$ *versus* $T$ relationship; (a) glassy state, (b) paramagnetic species in glassy state, and (c) phase III.

magnetic data. In the figures the melting points of each sample obtained from the magnetic study are fitted to those from the thermal study.

$\chi_m$ of phase III decreases with increasing temperature according to the characteristic behavior of paramagnetic substances (Fig. 7). Although a slight fall in $\chi_m$ occurred at the transition point corresponding to phase III→I, the magnetic property of the new phase I was found to be paramagnetic similar to phase III. At melting point $T_m$, the value of $\chi_m$ decreased abruptly by one half, but in the liquid state $\chi_m$ was nearly independent of the temperature.

In the heating curve of $\chi_m$ for phase IV (Fig. 8), the value of $\chi_m$ increases sharply at the transition point and the diamagnetic phase IV is transformed into a paramagnetic phase I. The melting behavior is quite the same as that shown in Fig. 7.

In the cooling curve of $\chi_m$ for the molten substance (Fig.9), the liquid and the supercooled liquid states show paramagnetism but the magnetic behavior is peculiar. Upon cooling to the glass transition point $T_g$, the values of $\chi_m$ decrease but are almost independent of temperature. Below $T_g$, however, $\chi_m$ seems to obey roughly the Curie law.

In the heating curve of $\chi_m$ for the glassy state (Fig.10), magnetic susceptibility up to $T_g$, shows an ordinary paramagnetism except in the vicinity of $T_g$. Above $T_g$, the behavior of $\chi_m$ is characteristic of the supercooled liquid state. The value $\chi_m$, however, decreases suddenly at crystallization temperature and shows diamagnetism in the new phase II. On further heating, the diamagnetic phase II is transformed into a paramagnetic phase *via* complicated steps of transition and finally melts at 460 K.

The effective Bohr magneton number $\mu_{eff}$ of phases I, III, and the glassy state is given in Table 3. It

Table 3. Effective Bohr magneton number of Ni(3-$CH_3O$-SAL·*iso*-$C_3H_7)_2$ $\mu_{eff}=2.83\sqrt{\chi_a(T-\theta)}$

| $T$/K | $\mu_{eff}/\mu_B$ | | $T$/K | $\mu_{eff}/\mu_B$ | | $T$/K | $\mu_{eff}/\mu_B$ | |
|---|---|---|---|---|---|---|---|---|
| | Phase I | | | Apparent $\mu_{eff}$ of glassy state | | | $\mu_{eff}$ of paramagnetic species | |
| | $\theta=0$ | | | $\theta=0$ | $\theta=+21$ | | in glassy state | |
| 437 | 3.15 | | 133 | 1.89 | 1.74 | | $\theta=0$ | $\theta=+21$ |
| 449 | 3.18 | | 151 | 1.90 | 1.74 | 133 | 3.59 | 3.25 |
| | | | 169 | 1.88 | 1.74 | 151 | 3.58 | 3.25 |
| | Phase III | | 185 | 1.85 | 1.74 | 169 | 3.54 | 3.25 |
| | $\theta=0$ | $\theta=-54$ | 201 | 1.84 | 1.74 | 185 | 3.46 | 3.25 |
| 297 | 3.17 | 3.46 | 218 | 1.82 | 1.74 | 201 | 3.42 | 3.25 |
| 331 | 3.17 | 3.46 | 234 | 1.82 | 1.74 | 218 | 3.37 | 3.25 |
| 342 | 3.18 | 3.46 | 251 | 1.83 | 1.74 | 234 | 3.36 | 3.25 |
| 363 | 3.21 | 3.46 | 267 | 1.81 | 1.74 | 251 | 3.35 | 3.25 |
| 387 | 3.24 | 3.46 | 282 | 1.78 | 1.74 | 267 | 3.30 | 3.25 |
| 412 | 3.24 | 3.46 | | | | 282 | 3.23 | 3.25 |

has been calculated on the basis of both the Curie law, $\mu_{eff}=2.83\sqrt{\chi_a T}$, and the Curie-Weiss law, $\mu_{eff}=2.83\sqrt{\chi_a(T-\theta)}$, the atomic magnetic susceptibility $\chi_a$ being determined by correcting the underlying diamagnetism of all constituent atoms ($-267\times10^{-12}$ $m^3mol^{-1}$). The Weiss constants of phase III and of the glassy state were determined from Fig.11 to be $-54$ K and $+21$ K, respectively. It was impossible to estimate the Weiss constant of phase I because of the limited temperature region. The signs of the constant imply that the intermolecular interactions in the glassy state and in phase III have a ferromagnetic and antiferromagnetic nature, respectively. The values of the Weiss constants for both cases, however, seem to be extraordinarily large in view of the fact that the Weiss constant is proportional to the interaction between magnetic ions in molecular field theory. In the glassy state, the packing of molecules may be somewhat loose as compared with a crystalline phase and the regular superexchange paths established in a crystalline phase may be disturbed randomly in the glassy state. Therefore, a small value for the Weiss constant is expected for the glassy state. The interpretation for the large Weiss constant obtained by the present experiment will be a further problem. The Weiss constant for phase III, $\theta=-54$ K, indicates the existence of a heat capacity anomaly or a magnetic phase transition at a temperature of several tens degree-Kelvin. However, such a heat capacity anomaly was not found down to 13 K. Further discussions concerning the magnetic interaction will not be given, since a small uncertainty in temperature and a large extrapolation from the high temperature will lead to errors.

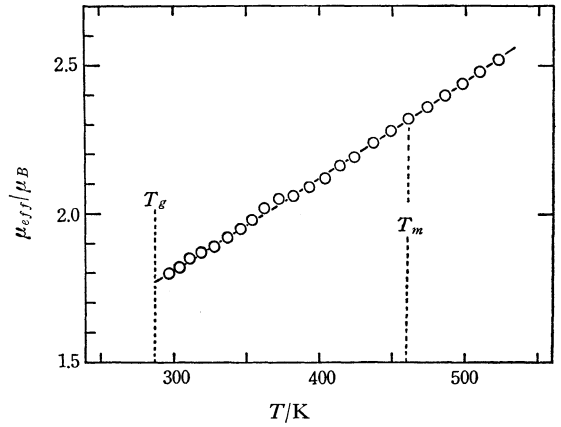


Fig. 12. Effective Bohr magneton number of supercooled liquid against temperature.

The effective Bohr magneton number of the supercooled liquid state is shown in Fig.12 as a function of temperature. An explanation of the magnetic susceptibilities of the molten nickel(II) complexes based on the existing equilibrium between the diamagnetic and the paramagnetic species has already been given.[12] We have applied a similar discussion to the present supercooled liquid and the glassy states of Ni(3-$CH_3O$-SAL·*iso*-$C_3H_7)_2$. In the supercooled liquid state, an equilibrium between two species seems to be established since the magnetic susceptibility shows a curious behavior and does not obey the Curie law. It is assumed here that a certain equilibrium may be reached between the paramagnetic tetrahedral molecule of phase III and the diamagnetic planar molecule of phase II and/or phase IV. The molar fraction of the paramagnetic species $x$ in the supercooled liquid state is related to the effective Bohr magneton number of phase III and that of the supercooled liquid state as follows.

$x$ = $\chi_a$(supercooled liquid state)/$\chi_a$(phase III)
= [$\mu_{eff}$(supercooled liquid state)]$^2$/[$\mu_{eff}$(phase III)]$^2$.

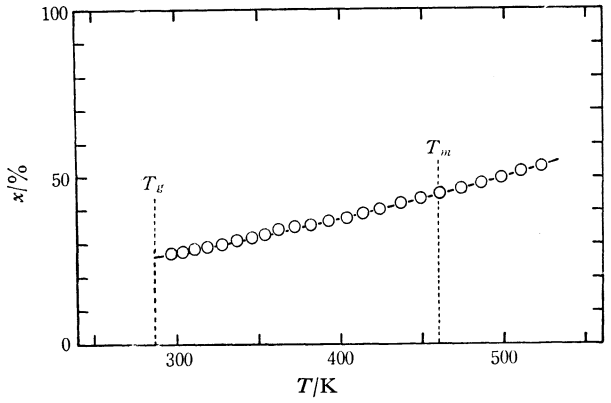


Fig. 13. Temperature dependence of the paramagnetic content in the liquid and the supercooled liquid states.

12) L. Sacconi, R. Cini, and F. Maggio, *J. Inorg. Nuclear Chem.*, **8**, 489 (1958).

The temperature dependence of $x$ is shown in Fig.13. Upon cooling down to $T_g$, the paramagnetic species are partially converted into a diamagnetic one according to the following equilibrium relationship.

$$\underset{(1-x)}{\text{diamagnetic species}} \rightleftarrows \underset{(x)}{\text{paramagnetic species.}}$$

The equilibrium constant $K_p$ was determined from the relation

$$K_p = [\text{paramagnetic species}]/[\text{diamagnetic species}] = x/(1-x).$$

The thermodynamic quantities $\Delta G$, $\Delta H$, and $\Delta S$ associted with this equilibrium can be calculated from the plot of $\ln K_p$ against $1/T$ as shown in Fig.14. The numerical values are listed in Table 4. As was expected the free energy difference between the two species is rather small. This may be one reason why two crystalline forms can be obtained stably from different solvents. The free energy data also show that at lower temperatures the diamagnetic planar form is more stable than the paramagnetic tetrahedral one, but at higher temperatures such as 510 K, the order of stability is reversed. Both $\Delta H$ and $\Delta S$ are considerably small compared with those of other solutions of Schiff base metal complexes.[4] Steric effects of the substituent groups and solvent effect will be responsible for this difference.

In the glassy state, however, the conversion of the paramagnetic species into the diamagnetic one seems to be frozen because of a long relaxation time required. The content of the paramagnetic species in the glassy state was estimated from Fig.13 to be about 26%. The magnetic susceptibility of the glassy state obeys the Curie law in keeping the paramagnetic content at 26%. This behavior seems to be consistent with the thermodynamic nonequilibrium condition in the glassy state. By using the paramagnetic content of *ca.* 26% the experimental susceptibility data in the glassy state was reduced to the molar paramagnetic susceptibility. In this case the Weiss constant also becomes +21 K (Fig. 11).

As is shown in Fig.10, the magnetic susceptibility around the glass transition temperature varies continuously with temperature with no jump. This is in contrast to other phase transition regions. In the temperature range from about 232 K to $T_g$, an approximately linear relationship holds between the magnetic susceptibility and temperature for the glassy state. This may be partially due to the enthalpy relaxation effect, which is generally observed just below the glass transition point. In other words, in setting the sample at this temperature region for a long time, its magnetic susceptibility decreases gradually to the extrapolated value from the supercooled liquid state.

Table 4. Thermodynamic quantities for diamagnetic ⇄ paramagnetic equilibrium in the supercooled liquid state of Ni(3-$CH_3O$-SAL·*iso*-$C_3H_7)_2$

| $T$/K | $\Delta G$ / kJ mol$^{-1}$ | $\Delta H$ / kJ mol$^{-1}$ | $\Delta S$ / J K$^{-1}$ mol$^{-1}$ |
|---|---|---|---|
| 304 | 2.43 | 3.82 | 4.56 |
| 337 | 2.27 | 3.89 | 4.81 |
| 404 | 1.72 | 7.15 | 13.5 |
| 437 | 1.19 | 8.83 | 17.5 |
| 474 | 0.552 | 9.50 | 18.9 |
| 510 | −0.238 | 11.3 | 22.6 |

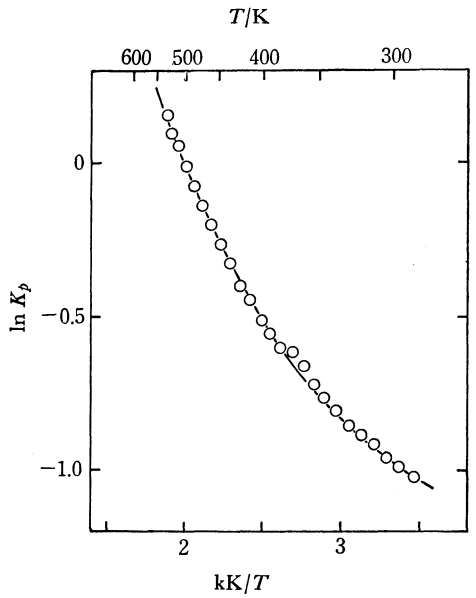


Fig. 14. Temperature dependence diamagnetic ⇄ paramagnetic equilibrium constant in the supercooled liquid state.

## Conclusion

Thermal and magnetic properties of Ni(3-$CH_3O$-SAL·*iso*-$C_3H_7)_2$ were investigated by means of various methods. In addition to the known crystalline phases III and IV, two new crystalline phases I and II and the existence of the supercooled liquid and the glassy states were found. The molecular structure and its associated magnetic properties in phases I and II were determined to be of paramagnetic tetrahedral form and diamagnetic square-planar one, respectively. The infrared and electronic spectra elucidated that the molecular configuration in phase I resembles that in phase III and that the molecular form in phase II is similar to that in phase IV. However, remarkable differences were observed in the heat of solution data between phases I and III, and between phases II and IV. These facts imply that the spectroscopic methods reflect the local symmetry in a molecule, or that information on short-range effects can be obtained from the spectroscopic methods. The calorimetric methods reveal the intermolecular or the long-rang effects in a condensed system.

The unusual magnetic behavior observed in the supercooled liquid state was well accounted for by assuming that an equilibrium between the paramagnetic and the diamagnetic species is established. In decreasing temperature the paramagnetic species was partially converted into the diamagnetic one. But further cooling below glass transition temperature prevented the conversion between two species because of a much longer relaxation time. In the glassy state the para-

magnetic content was found to be about 26% and its magnetic susceptibility obeyed the Curie-Weiss law.

From the viewpoint of statistical mechanics the paramagnetic glass will provide an interesting problem. The present glassy state may be regarded as a random-system in which the paramagnetic species are distributed randomly. The question, whether any phase transition will occur or not in such a random-system, remains unsolved. To obtain more insight into this problem it will be necessary to measure exactly the magnetic susceptibility of the glassy state down to a further low temperature region.

The magentic measurements of the paramagnetic phases I and III at lower temperature will also provide the detailed knowledges about the Weiss constants and the nature of the intermolecular interactions.

The authors would like to express their sincere thanks to Professor Y. Shimura and Dr. S. Kaizaki who kindly permitted use of the spectrophotometer to obtain the electronic spectra, and to Professor A. Tazaki and Mr. G. Kaji, Faculty of Engineering Science, for the use of the apparatus for magnetic susceptibility measurements.